J. Adhesion, 1995, Vol. 53, pp. 69–78
Reprints available directly from the publisher
Photocopying permitted by license only

Transient Thermal Deformations of the Interphase in Polymer Composites*

N. R. SOTTOS and M. SWINDEMAN

Department of Theoretical and Applied Mechanics, University of Illinois at Urbana-Champaign, Urbana, IL 61801, USA

(Received August 22, 1994; in final form February 15, 1995)

Heterodyne micro-interferometry was utilized to measure out-of-plane transient displacements in the interphase due to thermal cycling. In-situ measurements were made on single carbon fiber/epoxy samples with interphases of varying glass transition temperature. Interphase properties were tailored such that one set of samples had fibers which were coated with a low T_g resin, another set had a higher T_g coating, and in the third set the fibers were uncoated. The interferometric data demonstrated that interphase T_g has a significant effect on the rate and magnitude of the thermal deformations at the fiber/matrix interface. The presence of a low T_g interphase caused an increase in the magnitude of the thermal displacements due to a local softening of the matrix and increase in coefficient of thermal expansion. In addition, the rate at which the displacements increase was also higher due to the reduction in T_g. Samples with untreated fibers (no tailored interphase) behaved as if a low T_g interphase had formed. Experimental displacement profiles were also compared with finite element predictions to assess the behavior of the tailored interphases.

KEYWORDS: fiber/matrix interface; tailored interphases; transient thermal deformations; interphase glass transition; interferometry; polymer composites

1 INTRODUCTION

Many of the overall thermo-mechanical properties of a composite material are influenced by the local structure and properties of an interphase region developed at the fiber/matrix interface. In polymer matrix composites, several researchers have found evidence of an interphase with a glass transition temperature that is significantly lower than that of the neat resin. Pogany[1] first showed that non-stoichometric concentrations of an aliphatic polyamine crosslinked with an epoxy resin can lead to reductions in the glass transition temperature. Lipatov *et al.*[2] concluded a selective sorption of one of the components in a filled epoxy system may occur on the filler surface before hardening. A surplus of the other component may act as a plasticizer which causes a reduction of elastic moduli and a change in the relaxation behavior of the filled system. Crowson and Arridge[3] observed a difference in glass transition temperature between filled and unfilled epoxy systems. In addition, Papanicolaou, *et al.*[4] discussed the existence of a viscoelastic interphase with a lower glass transition temperature.

---

*One of a Collection of papers honoring Lawrence T. Drzal, the recipient in February 1994 of *The Adhesion Society Award for Excellence in Adhesion Science, Sponsored by 3M.*

More recently, Palmese and McCullough[5] showed that a stoichiometric imbalance of epoxy resin and amine curing agent develops near graphite fiber surfaces. The cross-link density, epoxy concentration and amine concentration were predicted as a function of radial distance from the fiber surface. Changes in glass transition temperature were then measured for the predicted amine concentrations using both dynamic and thermal mechanical analysis (DMA and TMA). For amine concentrations both above and below the stoichiometric point, the value of T_g was significantly reduced. Since the fiber surface alters the cure chemistry such that a non-stoichometric mixture of amine and epoxy occurs, the polymer in that region was predicted to have a much lower T_g than the neat resin.

Interferometric measurements reported by Sottos *et al.*[6,7] also support the existence of an interphase region with a reduced glass transition temperature. Steady-state thermal displacement profiles were measured using a scanning micro-interferometer for samples consisting of a single carbon fiber embedded in an epoxy matrix. Comparison of experimental profiles measured by the interferometer with theoretical displacement predictions indicated that the value of the matrix properties near the fiber surface differed appreciably from their value in the neat resin. The difference between the experimental and theoretical curves when no interphase was considered was too large to be accounted for by experimental error or small variations in the properties of the matrix. A thin interphase region of approximately 0.06 fiber radii, with a modulus an order of magnitude lower than the neat resin, most closely matched the experimental profiles. In order for the modulus to be this low, the epoxy in this region would have to be heated to a temperature above its glass transition.

Further experimental evidence of a reduced glass transition temperature in carbon epoxy composites has been reported by Rao and Drzal,[8] Skourlis and McCullough,[9] and Sottos and Li.[10] In these investigations, single fiber fragmentation tests were performed over a range of temperatures. A significant decrease in interfacial shear strength (IFSS) was observed at temperatures far lower than the glass transition of the matrix, indicating the presence of an interphase with different properties. Sottos and Li[10] performed the fragmentation tests for fibers with a tailored interphase of known glass transition. Reductions in interfacial shear strength were found to correlate with the T_g of the fiber coating. Samples with a higher T_g interphase showed only a 10% reduction in IFSS at 100°C, while samples with a low T_g had a 26% reduction in IFSS. Uncoated fibers (no tailored interphase) showed nearly the same reduction in IFSS as the low T_g interphase samples at 100°C. The results strongly indicated the formation of an interphase with a reduced T_g in uncoated carbon/epoxy systems.

The existence of a reduced T_g has significant implications for the thermal behavior and long term performance of a composite. The single fiber fragmentation studies[8,9,10] have shown that the interfacial shear strength and the ability to transfer load significantly decrease at temperatures near the T_g of the interphase. Hiemstra and Sottos[11] and Sottos *et al.*[7] investigated the effects of the interphase on thermally-induced microcracking. Both the initiation and location of interfacial microcracks were correlated with interphase T_g. Microcracks occurred at the lowest thermal load in samples with a higher T_g at the fiber/interphase interface. In samples with a low T_g interphase, microcracks initiated at higher thermal loads and at the interphase/matrix interface. The presence of the low T_g coating prevented cracks from reaching the fiber surface.

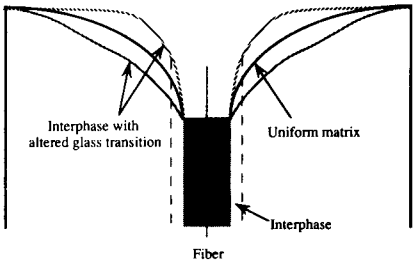

FIGURE 1 Schematic of single fiber thermal displacement for a uniform temperature change.

In the current work, the influence of interphase glass transition on time and temperature behavior is investigated further. The formation or introduction of an interphase region with an altered glass transition temperature will significantly influence the local time-dependent deformation in that region. Transient thermal displacements are measured using micro-interferometry for the three different single fiber sample types considered in Sottos and Li.[10] Interphase properties are tailored such that one set of samples has fibers which are coated with a low T_g resin, another set has a higher T_g coating, and in the third set the fibers are uncoated. A schematic of the single fiber sample and resulting out-of-plane thermal displacements for a uniform temperature change is shown in Figure 1.

Heterodyne micro-interferometry is utilized to measure any changes in the transient displacement profiles due to the different interphase glass transition temperatures. This interferometric technique has been used previously to measure static displacements for uncoated and coated fibers[6,7] and is presently modified to acquire transient data. Experimental displacement profiles are compared with finite element predictions to assess the viscoelastic behavior of the tailored interphases.

2 SAMPLE PREPARATION

Single carbon fiber/epoxy samples were prepared with three different types of interphases. The fibers used for this study were untreated, pitch-based carbon fibers supplied by Textron. All fibers were washed in isopropyl alcohol to remove any surface lubricants or contaminants and allowed to dry. Shell EPON 828® (diglycidyl ether of bisphenol A) resin cured with AMICURE® PACM [bis (p-amino cyclohexyl) methane] was chosen for the matrix material. In the first type of sample (type I), the fibers were left uncoated. For the second type of sample (type II), fibers were coated with a thin layer of EPON 871® resin to reduce the glass transition and modulus of the interphase. EPON 871 (aliphatic polyepoxide) is an amber, low viscosity liquid which imparts increased flexibility to EPON 828 compositions. The fibers were coated by gently pulling single filaments through a bath of the resin. For the third type of sample (type III), fibers were coated with a thin layer of a stoichiometric mix of EPON Resin DPS-164 (epoxy cresol novolac) and PACM. An interphase with a glass transition temperature of 150°C and slightly higher modulus was obtained. The solid DPS 164 was first dissolved in acetone, then mixed with PACM. After evaporating the acetone, the coating was cured on the

TABLE I
Properties of Matrix and Coatings

Resin	E(GPa)	T_g(°C)	α(ppm)	
			$T < T_g$	$T > T_g$
Neat Matrix- (EPON 828 + PACM)	2.5	160	68	160
Coating II- (EPON 871 + 828 + PACM)	2.1	80	73	228
Coating III- (EPON DPS 164 + PACM)	3.5	150	72	175

fibers. The Young's modulus measured by room temperature tensile tests, coefficient of thermal expansion obtained by TMA (Thermal Mechanical Analysis) and glass transition temperature measured by DSC (Differential Scanning Calorimetry) for the matrix and coatings are listed in Table I.

Samples were fabricated by placing a single carbon fiber, coated or uncoated, into the center of a mold which was then filled with a stoichiometric mix of resin (28 parts PACM to 100 parts EPON 828). All samples were held for 1 hour at 80°C to minimize the bubbles in the resin phase, then cured for 1 hour at 150°C, and allowed to cool slowly to room temperature overnight. Specimens were cut to a length of approximately 1.5 cm and the front and back faces were polished metallographically. In addition, a thin layer of gold was sputtered onto the surface to provide both a current conduction path and a highly reflective surface. The radius of the fiber was determined to be exactly $r_1 = 17.5\,\mu m$ from a photomicrograph of the sample surface. The outer radius of the samples measured $r_2 = 15.875\,mm$.

3 EXPERIMENTAL PROCEDURE

Heterodyne micro-interferometry was utilized to study differences in transient thermal displacements caused by changing the interphase glass transition temperature. This interferometric technique has been used previously to measure static displacements for uncoated and coated fibers[6,7] and is presently modified to acquire transient data.

A detailed description of the interferometric experimental technique utilized for the displacement measurements is given by Sottos *et al.*[12] A single, linearly-polarized light beam from an Argon laser is incident upon a 40 MHz acousto-optic modulator (AOM) producing two beams which are sent along different arms of the interferometer. The first beam (reference beam) propagates with the same frequency as the beam incident upon the AOM. The second beam is shifted in frequency by 40 MHz and is used to illuminate the sample surface. The two beams are recombined in a beam-splitter and then arrive at the primary lens of a long distance microscope. An image is formed behind the microscope and is magnified onto the image plane of a scanning photodiode detector using an eyepiece lens. The light that forms the sample image differs in frequency by 40 MHz from the light that forms the reference image. Thus, any z-axis displacement of the sample surface will produce phase shifts in the 40 MHz beat signal arriving at the photodetector. A lock-in amplifier is used to compare the phase of the 40 MHz signals from both the reference and the scanning detectors. This technique has

the capability of measuring thermal displacements with an out-of-plane resolution of 50 angstroms and a possible in-plane resolution of 0.5 microns.

Samples were mounted in the interferometer with the embedded fiber parallel to the incoming beam. To heat the sample, a 12.0 mA current was passed through the fiber. A repeatable, radial temperature field was generated with minimal convection of heat into the interferometer path, minimizing thermal effects on the apparatus. The transient temperature field in the sample can be predicted analytically or using finite elements with good agreement. Temperature profiles predicted using the finite element method are plotted in Figure 2 as a function of radial distance, $\rho = r/r_1$. The fiber and matrix thermal conductivity, K, and thermal diffusivity, κ, used for the calculations are given in Table II. The temperature at the fiber/matrix interface increases over 22°C in less than 5 sec for a power input per unit volume of 7.07×10^9 W/m^3. As expected, the temperature gradient decreases rapidly with radial distance.

Data acquisition was triggered by the application of voltage across the sample and displacement (phase) data were stored during the first 4.5 seconds of heating. Transient displacement profiles were obtained at various radial locations out from the fiber center. In Figure 3, axial displacement is plotted as a function of time and radial

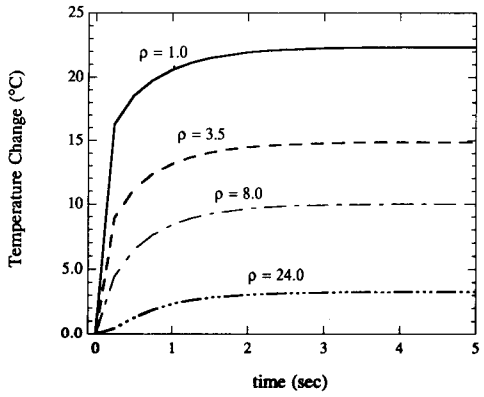

FIGURE 2 Finite element predictions of the transient temperature profile (ΔT) at various radial locations for a power input of 7.07×10^9 W/m^3.

TABLE II
Fiber and Matrix Material Properties

Property	Carbon Fiber	EPON 828/PACM
E(GPa)	41.0	2.5
α (ppm)	−0.5	68.0
$K\left(\frac{W}{m°C}\right)$	8.36	0.180
$\kappa\left(\times 10^{-6}\frac{m^2}{s}\right)$	0.1414	5.728
ν	0.22	0.33

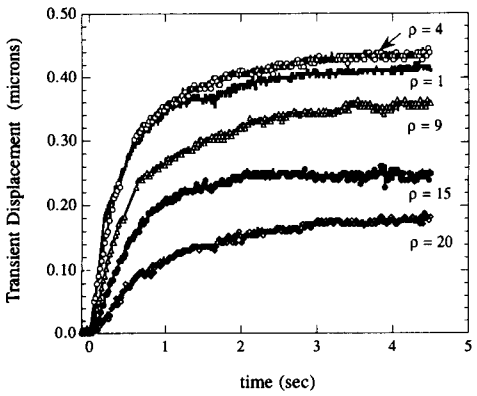

FIGURE 3 Transient displacement profiles at various radial locations for sample type I.

position for sample type I (no interphase). Similar to the temperature profiles in Figure 2, the displacement profiles are quite steep near the fiber/matrix interface. A maximum transient displacement of 0.44 microns occurs at 4.0 fiber radii from the fiber center and then decreases with increasing radial distance. The maximum displacement occurs close to the interface due to the non-uniform heating of the matrix. Displacement measurements were repeated for the other two samples and are discussed below.

4 ANALYSIS OF INTERPHASE BEHAVIOR

Comparison of Different Interphase Types

In this section, displacement measurements are compared at various radial locations for the three different sample types. Transient displacement profiles at the fiber/matrix interface ($\rho = 1$) are plotted in Figure 4. The interphase type has a significant effect on

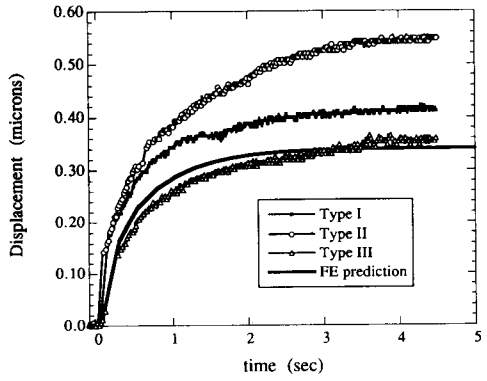

FIGURE 4 Comparison of transient displacement profiles at the fiber/matrix interface ($\rho = 1$) for sample types I, II and III.

the magnitude and rate of the thermal displacements. The low T_g sample (type II) has the largest maximum displacement, while the higher T_g (type III) sample has the smallest. As the radial distance is increased away from the interface, the displacement profiles for the different sample types begin to converge. Displacements at $\rho = 1.3$, 5 and 15 are plotted in Figures 5–7, respectively. At $\rho = 1.3$, the initial displacement for the three samples is decreased slightly from the value at $\rho = 1$ and the profiles are closer together. At a radial distance of $\rho = 5$, the experimental displacements curves are all nearly the same. In the far field at $\rho = 15$, the curves have collapsed to the same values as may be anticipated.

Comparison with Finite Element Predictions

The experimental profiles in Figure 4–7 were compared with finite element predictions to better assess the influence of interphase properties. An axisymmetric finite element

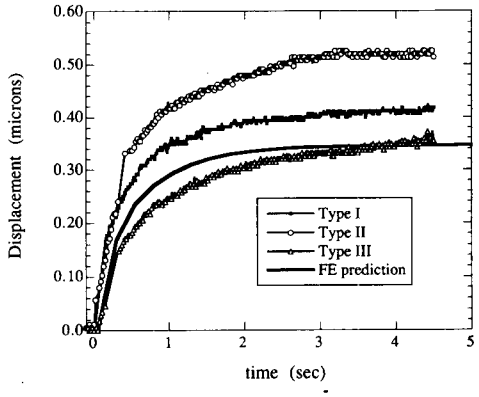

FIGURE 5 Comparison of transient displacement profiles at $\rho = 1.3$ for sample types I, II and III.

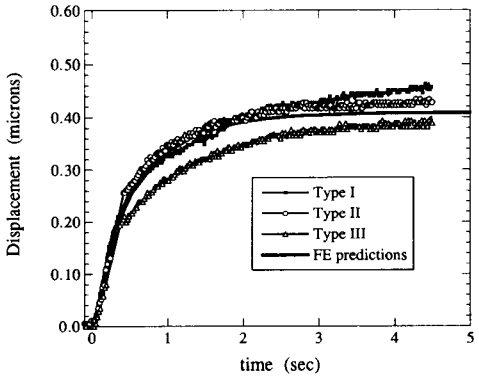

FIGURE 6 Comparison of transient displacement profiles at $\rho = 5.0$ for sample types I, II and III.

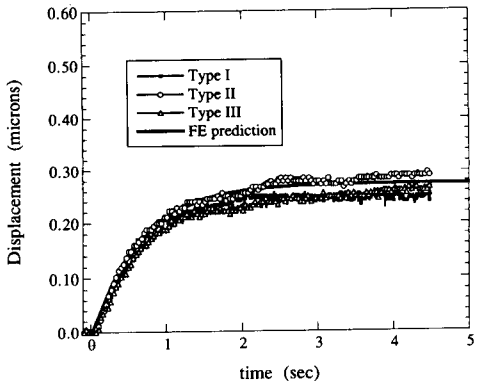

FIGURE 7 Comparison of transient displacement profiles at $\rho = 15.0$ for sample types I, II and III.

model of the single fiber sample was generated and analyzed using ABAQUS© software. This model was 40 fiber radii in depth and length, employing 937 CAX8RT (quadratic, axisymmetric, reduced-integration, coupled thermal-displacement) elements and 4697 nodes. The mesh was finest at the top surface and along the fiber matrix interface where the elements were approximately 1/8 fiber radii in both dimensions. By using quadratic MPC's for mesh refinement, the maximum element aspect ratio was maintained at 10. In the transient analysis, the time increment was maintained at 10 msecs over the first 0.1 secs of heating and then increased to 50 msecs.

Covergence was based on a series of several models. Results from models where the finest elements were of 1/4, 1/8, and 1/16 of a fiber radius were compared. Time step sensitivity was also evaluated by comparing models with time incrementation of 1, 0.5, 0.1, 0.05, 0.01, and 0.005 seconds. The particular model chosen (time step = 0.01 sec, finest element = 1/8 fiber radii) optimized accuracy with consideration to computational time. All calculations were made assuming perfect fiber/matrix interface bonding and uniform matrix properties (no interphase). Necessary elastic properties of the fiber and matrix are given in Table II.

The experimental profiles and finite element predictions are in excellent agreement from about 5 fiber radii out to the far field matrix. At closer than 5 fiber radii to the fiber center, all of the curves start to differ dramatically. The experimental displacement values for sample types I and II are significantly higher than predicted by finite elements for a uniform matrix with no interphase. Profiles for sample type III, however, are in fairly good agreement with the computational predictions.

Figure 8 shows a close up of the data taken at the fiber/matrix interface ($\rho = 1$) during the first second of heating. Both type I (no interphase) and type II samples show a rapid increase in displacement at small times, while the rise is less steep for type III. Although sample type I has no tailored interphase and the neat matrix has a high T_g (see Table I), the matrix material near the fiber surface does not behave as predicted for a uniform matrix. In fact, the time-dependent behavior is more similar to sample II which has a tailored low T_g interphase. The displacement profiles for sample III which has a tailored interphase T_g close to that of the neat resin are in good agreement with the finite element predictions for the case of no interphase.

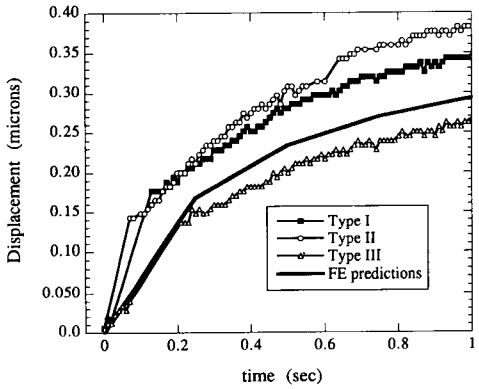

FIGURE 8 Enlarged view of the initial transient displacement at the fiber/matrix interface ($\rho = 1$) for sample types I, II and III.

These results are consistent with previous investigations which have demonstrated the existence of a low T_g interphase region for untreated carbon fibers in epoxy.[6-10] The modulus and coefficient of thermal expansion of the low T_g and higher T_g coatings are fairly close in value and not that much different than that of the matrix (See Table I) at temperatures below the glass transition. Thus, the difference in displacement profiles between the different samples in Figures 4 and 8 are largely due to an increase in expansion coefficient and local softening of the matrix as sample type II is heated very close to its glass transition. Sample type III does not demonstrate such an increase in displacement because the T_g is tailored to be much higher than the heating temperature. The similarity in behavior between sample types I and II suggests that Type I is also exceeding its glass transition locally. Thus, the interphase glass transition temperature has a significant effect on the magnitude and rate of the thermal displacements. In addition, the data support the formation of a low T_g interphase for untreated fibers.

5 DISCUSSION AND CONCLUSIONS

The existence of a reduced glass transition temperature in the interphase may significantly influence the viscoelastic behavior of a composite. Papanicolaou *et al.*[4] reported that the interphase in polymer matrix composites is viscoelastic. Gosz *et al.*[13] investigated the effect of a viscoelastic interface layer on the mechanical behavior of a transversely-loaded composite using finite elements. Stress distributions were found to change substantially as the effective stiffness of the interface decreased. Hashin[14] used a correspondence principle to investigate the influence of a viscoelastic interphase on creep and relaxation in polymer composites. The analysis demonstrated that the viscoelastic effect is significant for axial and transverse shear relaxations in unidirectional composites. Yi *et al.*[15] have predicted the influence of a distinct viscoelastic interfacial layer on the mechanical properties of laminated composites. Sancaktar *et al.*[16] has developed an analytical methodology to describe the viscoelastic effects on interphase strength observed during single fiber fragmentation tests.

The interferometric data presented in this paper demonstrates that interphase T_g has a significant effect on the rate and magnitude of the thermal deformations at the fiber/matrix interface. The transient displacement profiles are highly sensitive to changes in interphase glass transition, making the technique useful for characterizing time-dependent behavior in the interphase. The presence of a low T_g interphase causes an increase in the displacement magnitude due to a local softening of the matrix and an increase in thermal expansion coefficient. In addition, the rate at which the displacements increase is also higher because of the reduction in T_g. Samples with untreated fibers (no tailored interphase) behave as if a low T_g interphase had formed. For the case of a of higher T_g interphase, the rate of deformation and magnitude of the profiles are both reduced. The measurements reported may provide useful data for current and future micromechanical models of interphase time- and temperature-dependent behavior.

Acknowledgements

The authors gratefully acknowledge the support of the Office of Naval Research under grant N00014-92-J-1620. The assistance of Tom Keane in helping prepare samples is also greatly appreciated.

References

1. G. A. Pogany, *J. Mater. Sci.*, **4,** 405 (1969).
2. Y. S. Lipatov, V. F. Babich and V. F. Rosovizky, *J. Appl. Polym. Sci.*, **20,** 1987 (1976).
3. R. J. Crowson and R. G. C. Arridge, *Journal of Materials Science*, **12,** 2154 (1977).
4. G. C. Papaniclaou, S. A. Paipetis and P. S. Theocaris, *Colloid and Polymer Science*, **256,** 625 (1978).
5. G. R. Palmese and R. L. McCullough, *J. Polym. Sci.*, **46,** 1863 (1992).
6. N. R. Sottos, R. L. McCullough and W. R. Scott, *Composites Sci. Technol.*, **44,** 319 (1992).
7. N. R. Sottos, D. L. Hiemstra and W. R. Scott, in F. Erdogan and R. J. Hartranft, Eds., *Fracture Mechanics: 25th Volume*, **ASTM STP 1220** (ASTM, Philadelphia, 1995).
8. V. Rao and L. T. Drzal, *J. of Adhesion*, **37,** 83 (1992).
9. T. P. Skourlis and R. L. McCullough, *Composite Sci. Technol.*, **49,** 363 (1993).
10. N. R. Sottos and L. Li, *J. Adhesion*, **45,** 105 (1994).
11. D. L. Hiemstra and N. R. Sottos, *J. Composite Mater.*, **27,** 1030 (1993).
12. N. R. Sottos, W. R. Scott and R. L. McCullough, *Experimental Mechanics*, **31,** 98 (1991).
13. M. Gosz, B. Moran and J. D. Achenbach, *International J. Solids and Structures*, **27,** 1757 (1991).
14. Z. Hashin, *Mechanics of Mater.*, **11,** 135 (1991).
15. S. Yi, G. D. Pollock, M. F. Ahmad and H. H. Hilton, *AIAA Journal*, Paper No. 93-1517, to appear (1995).
16. E. Sancaktar, A. Turgut and F. Guo, *J. Adhesion*, **38,** 91 (1992).